ELSEVIER

Polymer 42 (2001) 5275–5283

polymer

www.elsevier.nl/locate/polymer

Toughening of some high-temperature poly(arylene ether)s and a hydroxypoly(benzoxazole) by sol–gel generated rubbery particles

C. Kumudinie[a], J.K. Premachandra[a], J.E. Mark[a,*], T.D. Dang[b], M.R. Unroe[b], F.E. Arnold[b]

[a]*Department of Chemistry and the Polymer Research Center, The University of Cincinnati, Cincinnati, OH 45221-0172, USA*
[b]*Polymer Branch, Air Force Research Laboratory, AFRL/MLBP B654, Wright–Patterson Air Force Base, OH 45433-7750, USA*

Received 28 June 1999; received in revised form 18 October 2000; accepted 18 October 2000

Abstract

Some high-temperature polymers, specifically two poly(arylene ether)s and a hydroxy(benzoxazole) copolymer (HPBO), were toughened using dispersed rubbery phases generated by the sol–gel process. These rubbery phases were introduced using combinations of sol–gel precursors with varying numbers of alkyl groups. Scanning electron micrographs showed uniformly dispersed particles in these composite materials. In poly(arylene ether)s, a significant increase in toughness and ultimate elongation were achieved for samples prepared from relatively large amounts of sol–gel precursor with higher numbers of alkyl groups. In HPBO, samples having low levels of the rubbery phase, both toughness and ultimate elongation were increased with increasing amount of the rubbery phase. Improvements in these properties of the HPBO polymer are rather large compared to the poly(arylene ether)s. The results also demonstrated improved thermal properties and decreased water absorption.

Keywords: Sol–gel process; Poly(arylene ether); Poly(benzoxazole)

1. Introduction

The use of polymeric materials in the manufacture of aerospace structures has increased markedly in recent years. This is due to their many desirable characteristics in comparison to traditional aerospace materials such as the metals aluminum and titanium. Their most desirable attribute is the ability to combine high strength and stiffness with low density [1].

Of particular interest are 'high-performance polymers', which possess a combination of excellent mechanical properties such as high strength, high stiffness and high impact resistance, and maintain these properties at the extremes of temperature. Other properties such as low dielectric constants, chemical and solvent resistance, and low flammability of these polymers are also desired [2]. There is an increasingly high demand for such polymers in the aerospace industry for the projected manufacture of high-speed commercial transport aircraft [3]. For example, Boeing's market projections indicate a significant demand for civil aircraft carrying 250–300 passengers over distances up to 8000 km and flying at supersonic speeds between Mach 2.0 and 2.4. At such high speeds, the aircraft would be exposed to very high temperatures [2]. Thus low-density high-temperature polymeric composites, which will reduce total platform and payload weight and still allow performance at very high speeds are of greater interest.

Polycarbonate and poly(methylmethacrylate) thermoplastic polymers already provide excellent transparency and impact properties for current military aircraft canopies, windows and windscreens [4]. However, the use of these materials at very high temperatures is impossible because of their low softening temperatures and low thermal stabilities. Thus, transparent high-temperature polymers are considered as possible candidates for such applications as well [2]. These polymers contain aromatic or heteroaromatic units in their backbone and these units provide exceptional thermal and chemical stabilities. However, these units are rigid and can cause the polymers to exhibit high degrees of brittleness. Therefore, high-temperature polymers need to be toughened for applications in advanced structural composites and other neat-resin applications including canopies.

The technique of toughening a brittle polymer by introducing a rubbery second phase has been known for more than two decades. Simple physical blending of the polymer with a second rubbery phase, however, leads to a

* Corresponding author. Tel.: +1-513-556-9292; fax: +1-513-556-9239.
E-mail address: markje@email.uc.edu (J.E. Mark).

0032-3861/01/$ - see front matter
PII: S0032-3861(00)00823-5

material with poor mechanical properties and the dispersed phase can cause loss of transparency due to a coarse dispersed phase morphology and poor interfacial adhesion [5–7]. Compatibilization is needed to convert such immiscible blends into commercially useful products. An appropriate compatibilizer could be a block or graft copolymer with one portion identical to or miscible with the polymer phase. A successful compatibilizer will permit finer dispersion of the second phase during mixing, stabilize the structure and improve interfacial adhesion [8].

Various types of elastomers have been employed as the rubbery second phase providing toughening effects in both thermoplastics and thermosets [9–11]. Diene polymers such as natural rubber and its copolymers [12] involving monomers such as butadiene are frequently used as the rubbery phase to obtain toughening. Their unsaturated structures can be an advantage with regard to reactions providing bonding between the phases, but also cause losses in stability, especially at high temperatures. Therefore, there is considerable interest in using totally saturated elastomers.

In the present study, the high-temperature polymers investigated were two poly(arylene ether)s and a hydroxy(benzoxazole) copolymer and they were toughened using siloxane-type rubbery phases. Of particular interest here is the fact that poly(arylene ether)s have been evaluated as potential high-transparency materials [4]. On the other hand, the hydroxy functional group in the benzoxazole copolymer gives the added advantage that it can be used to facilitate the bonding between the two phases through the use of a bonding agent [13,14]. The siloxane-type rubbery phase was generated in situ using the sol–gel process.

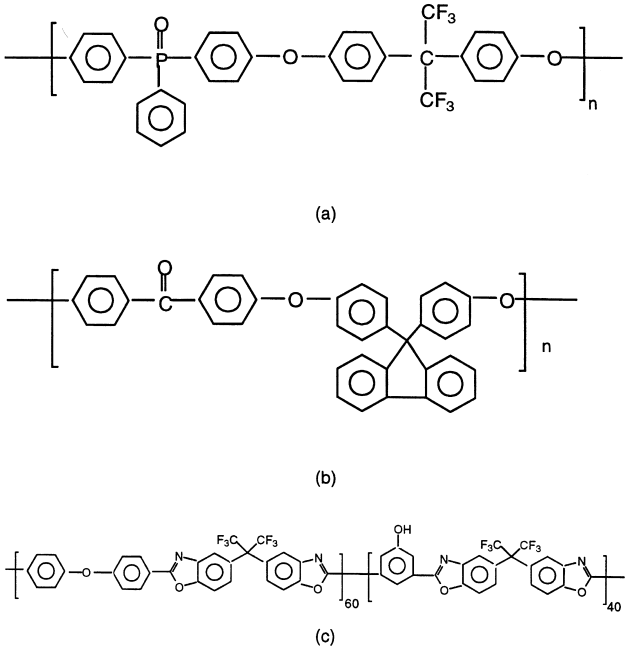

Fig. 1. Structures of the high-temperature polymers: (a) 6F-ETPP-E; (b) FEK-E and (c) HPBO.

This process [15] has been widely used to prepare organic–inorganic hybrid materials with unique combinations of properties from both organic and inorganic components [16]. In such cases, the organic polymer was reinforced by the secondary ceramic phase (e.g. silica). The preparation technique is based on the in situ generation of ceramic phases within the organic polymer by the sol–gel process using organometallic precursors such as tetramethoxysilane (TMOS) [16]. The two steps of the sol–gel process, hydrolysis and condensation, for TMOS are

$$Si(OCH_3)_4 + 4H_2O \rightarrow Si(OH)_4 + 4CH_3OH$$

$$Si(OH)_4 \rightarrow SiO_2 + 2H_2O$$

These reactions are catalyzed by acids, bases or salts [16]. Use of the sol–gel process for the preparation of organic–inorganic composites with high-temperature polymers as the organic phase [17,18], however, presents many difficulties. For instance, because of their intractability, most high-temperature polymers are virtually impossible to process. In addition, due to their unreactivity (which is desired in most of their applications), bonding between the organic polymer phase and the inorganic ceramic phase is generally not possible. This can cause phase separation with the resulting materials having properties less than expected. In order to enhance the processability, functionalized polymers, which are soluble in common organic solvents have been synthesized in recent years. In addition, using these functionalized polymers, the undesirable phase separation can be minimized by bonding the two phases through the use of a bonding agent [13,14,19,20].

The primary interest in the present research was to toughen brittle high-temperature polymers by a secondary rubbery phase. This was achieved by in situ generating organically modified silica structure by the sol–gel technique within the polymer matrix. More specifically, the brittleness of the silica particles, which are generally used to reinforce polymers, was reduced by incorporating alkyl groups into the generated particles. For this purpose, mixtures of sol–gel precursors alkyltrialkoxysilanes $R'Si(OR)_3$, dialkyldialkoxysilanes $R'R''Si(OR)_2$ and tetraalkoxysilanes $Si(OR)_4$ were used instead of $Si(OR)_4$ alone. Hydrolysis and condensation of $R'Si(OR)_3$ and $R'R''Si(OR)_2$ yield less rigid products since the particles contain non-hydrolyzable R' and R'' groups, which give the generated phases the deformability associated with toughness [21].

The resulting materials were characterized with regard to their structures, mechanical properties (modulus, ultimate strength, maximum extensibility, and toughness),

Table 1
Sample information for the 6F-ETPP-E composites

Designation	Dispersed phase (wt%)	TMOS:DMDMOS mole ratio
6F-ETPP-E-0	0	–
6F-ETPP-E-3:1	10	3:1
6F-ETPP-E-2:1	10	2:1
6F-ETPP-E-1:1	10	1:1
6F-ETPP-E-1:2	10	1:2
6F-ETPP-E-1:3	10	1:3

Table 2
Sample information for the FEK-E composites

Designation	Dispersed phase (wt%)	TMOS:DMDMOS mole ratio
FEK-E-0	0	–
FEK-E-3:1	10	3:1
FEK-E-2:1	10	2:1
FEK-E-1:1	10	1:1
FEK-E-1:2	10	1:2
FEK-E-1:3	10	1:3

thermal properties, optical properties, and tendencies to absorb water.

2. Experimental details

2.1. Materials

The polymers used as the continuous phase were two poly(arylene ether)s (designated 6F-ETPP-E and FEK-E), and a hydroxy(benzoxazole) copolymer (HPBO). The inherent viscosities at 0.2 g/dL in 1,1,2,2-tetrachloroethane at 30°C were 0.64 dL/g for the 6F-ETPP-E, and 0.94 dL/g for the FEK-E. The intrinsic viscosity of the HPBO in methanesulfonic acid, at 30°C was 1.0 dL/g. They were prepared at the Wright–Patterson Air Force Base [4] and their structures are shown in Fig. 1. The organosilanes tetramethoxysilane (TMOS) (99 + %), methyltrimethoxysilane (MTMOS) (99 + %), and dimethyldimethoxysilane (DMDMOS) (99 + %) were purchased from United Chemical Technologies, Inc. Anhydrous tetrahydrofuran (THF) was purchased from the Aldrich Chemical Company and diethylamine from Fisher, Inc. The bonding agent used for the HPBO polymer, isocyanatopropyltriethoxysilane (95%), was also purchased from United Chemical Technologies, Inc.

2.2. Sample preparation

2.2.1. Poly(arylene ether)s

The polymers 6F-ETPP-E and FEK-E were dried in a vacuum oven at 120°C to remove any water and the desired amount of each polymer was dissolved in anhydrous THF at the desired weight-to-volume concentration. After clear solutions were obtained, the chosen amounts of TMOS and DMDMOS were added. The mixtures were stirred at room temperature to again give clear solutions. Stoichiometric amounts of a 5 wt% diethylamine aqueous solution were then added and the mixtures were further stirred at room temperature to ensure homogeneous mixing. The resulting viscous solutions were transferred to Petri dishes for further hydrolysis and condensation. Evaporation of volatiles gave films, which were slowly dried in air. They were further dried under vacuum at 60°C for 2 days. A series of samples were thus prepared from each polymer by varying the amounts of sol–gel precursors. Preparative information is given in Tables 1 and 2.

2.2.2. Hydroxy(benzoxazole) copolymer

The procedure for preparing composites from the HPBO polymer is similar to that followed for the poly(arylene ether) composites. However, in the case of HPBO, after dissolving the polymer in anhydrous THF the bonding agent isocyanatopropyltriethoxysilane was added (in stoichiometric amounts relative to the number of OH groups in the copolymer). A series of samples with varying amounts of the dispersed secondary phase was thus prepared. These dispersed phases were generated within the polymer matrix by using different combinations of the sol–gel precursors, TMOS, MTMOS and DMDMOS. A summary of the information on the HPBO composite samples is given in Table 3.

2.3. Scanning electron microscopy

Scanning electron microscopy (SEM) was used to characterize both the film surfaces and their cross-sections. Specimens were coated with gold, mounted on aluminum mounts, and then examined using a Model 90 Cambridge instrument. Energy dispersive X-ray analysis (EDAX) measurements accompanied by silicon atom distribution maps on the same samples were obtained using an EDS system (Princeton Gamma Tech).

Table 3
Sample information for the HPBO composites

Designation	Dispersed phase (wt%)	Sol–gel precursors	
		TMOS:MTMOS mole ratio	TMOS:MTMOS:DMDMOS mole ratio
HPBO-0	0	–	–
HPBO-5-1:1	5	1:1	–
HPBO-15-1:1	15	1:1	–
HPBO-20-1:1	20	1:1	–
HPBO-5-1:1:1	5	–	1:1:1
HPBO-15-1:1:1	15	–	1:1:1
HPBO-20-1:1:1	20	–	1:1:1

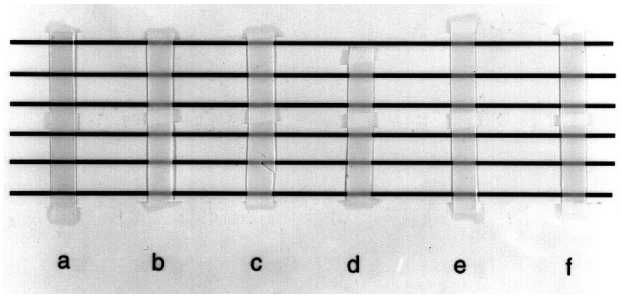

Fig. 2. Strips of the 6F-ETPP-E pure polymer and the toughened samples with 10 wt% rubbery phases demonstrating their transparencies: (a) pure polymer and the samples prepared from TMOS:DMDMOS mole ratios of (b) 3:1; (c) 2:1; (d) 1:1; (e) 1:2 and (f) 1:3.

2.4. Mechanical properties

Moduli, ultimate strengths and maximum extensibilities were measured at room temperature using an Instron mechanical tester. Samples with dimensions approximately $50 \times 5 \times 0.2\ mm^3$ were tested at a cross-head speed of 0.1 in/min.

2.5. Thermogravimetric analysis

Thermogravimetric analyses (TGA) were performed using a Perkin–Elmer model TAS-7 system at a heating rate of 20°C under a nitrogen atmosphere.

2.6. Water absorption

The extents of water absorption by the films under saturated conditions were measured by the method described in ASTM-D570-81. In brief, the films were dried at 120°C in vacuum overnight, weighed and immersed in distilled water, with periodic reweighings until the weight became constant.

3. Results and discussion

3.1. Morphology

In most cases, the samples had some transparency indicating good dispersion of the second phase. Fig. 2 shows this as a picture of vertically mounted strips of 6F-ETPP-E polymer with 10 wt% rubbery phase but with varying proportions of the sol–gel precursors used to generate the dispersed phase. Increasing the proportion of the flexibilizing DMDMOS is seen to decrease the transparency.

Figs. 3–5 show the scanning electron micrographs of unfractured and fractured surfaces of some selected samples. SEM pictures of the unfractured surfaces of the pure 6F-ETPP-E polymer and the sample having 10 wt% rubbery phase from 1:1 mole ratio of TMOS:DMDMOS are shown in Fig. 3(a) and (b), respectively. Fig. 3(b) shows well-dispersed uniform rubbery particles in the hybrid material. The particle distribution in the sample having 10 wt% rubbery phase from 1:3 mole ratio of TMOS:DMDMOS (Fig. 4) indicates that the particle size in this sample is larger than that in the sample with the same amount of rubbery phase generated using a 1:1 mole ratio of TMOS:DMDMOS. This could be due to the increased number of organic groups in the dispersed phase obtained from the 1:3 mole ratio of TMOS:DMDMOS compared to that from the 1:1 mole ratio. Fig. 5(a) and (b) shows the scanning electron micrographs of the fractured surfaces of the pure 6F-ETPP-E polymer and the sample having 10 wt% rubbery phase from the 1:1 mole ratio, respectively. As expected, the fractured surface of the sample having rubbery particles is somewhat coarse compared to that of the pure polymer.

The EDAX spectra for the 6F-ETPP-E pure polymer and that for the 6F-ETPP-E sample with 10 wt% rubbery phase from a 1:1 mole ratio of TMOS:DMDMOS are given in Figs. 6 and 7. The silicon distribution maps for the fractured and unfractured surfaces of the 6F-ETPP-E sample with 10 wt% rubbery phase from a 1:1 mole ratio of TMOS:DMDMOS are given in Fig. 8(a) and (b), respectively. Figs. 7 and 8 clearly show uniformly distributed silica confirming that the rubbery phase is dispersed homogeneously in the material.

3.2. Mechanical properties

Some of the mechanical properties of the 6F-ETPP-E pure polymer and the samples with 10 wt% rubbery phase prepared using varying TMOS:DMDMOS mole ratios are

Table 4
Mechanical properties of the 6F-ETPP-E composites

Rubbery phase		Modulus (MPa)	Ultimate strength (MPa)	Ultimate elongation (%)	Toughness (MPa)
Wt%	Sol–gel precursor[a]				
0	–	1820	35.3	4.3	1.17
10	TMOS:DMDMOS (3:1)	1900	24.4	1.2	0.18
10	TMOS:DMDMOS (2:1)	1940	33.4	2.7	0.59
10	TMOS:DMDMOS (1:1)	1940	34.0	9.4	2.69
10	TMOS:DMDMOS (1:2)	1580	36.3	6.7	2.05
10	TMOS:DMDMOS (1:3)	1370	32.8	10.4	2.81

[a] Molar ratios of the corresponding precursors are given in parentheses.

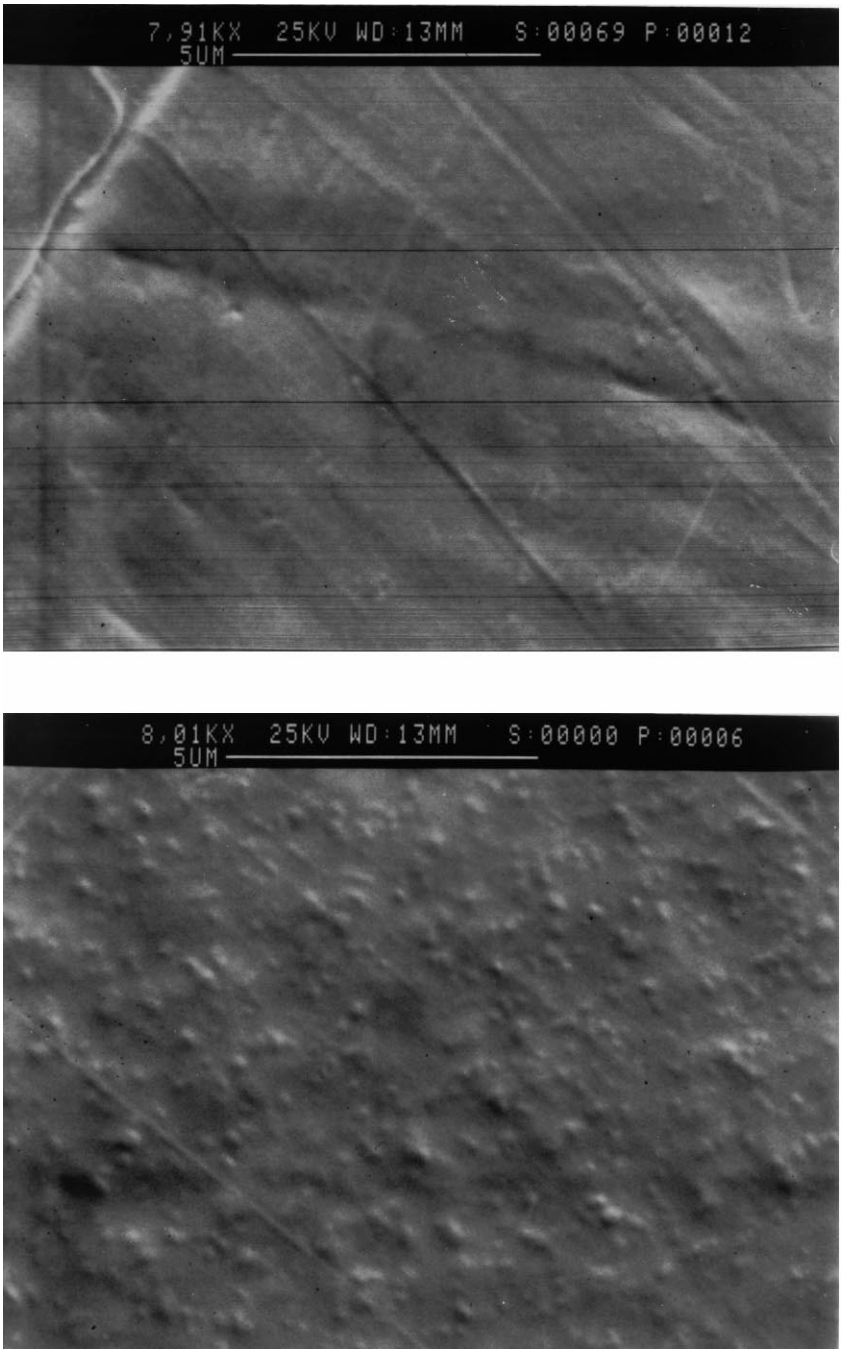

Fig. 3. Scanning electron micrographs for the unfractured surfaces of (a) 6F-ETPP-E pure polymer and (b) the sample with 10 wt% rubbery phase prepared from a 1:1 mole ratio of TMOS:DMDMOS.

described in Fig. 9 and Table 4. Compared to that of the pure polymer, the moduli of the samples from the 3:1, 2:1 and 1:1 mole ratios of TMOS:DMDMOS have been slightly increased, but those having 1:2 and 1:3 mole ratios have been decreased. The ultimate strengths of the samples with a rubbery phase have been slightly decreased compared to the pure polymer except for the sample corresponding to 1:2 mole ratio. Some substantial increases in ultimate elongation, however, have been obtained. As a result, the toughness as measured by the area under the stress–strain curve was increased for all the samples except for the samples from the 3:1 and 2:1 mole ratios. This decrease in the toughness and the ultimate elongation for the samples corresponding to these higher amounts of TMOS could have been anticipated since the relative amounts of glassy silica in the second phase were higher in these samples. The significant increases in toughness and ultimate elongation and the decrease in moduli for the samples prepared from 1:2 and 1:3 mole ratios are all presumably due to the considerable increase in the rubbery properties of the silica particles from

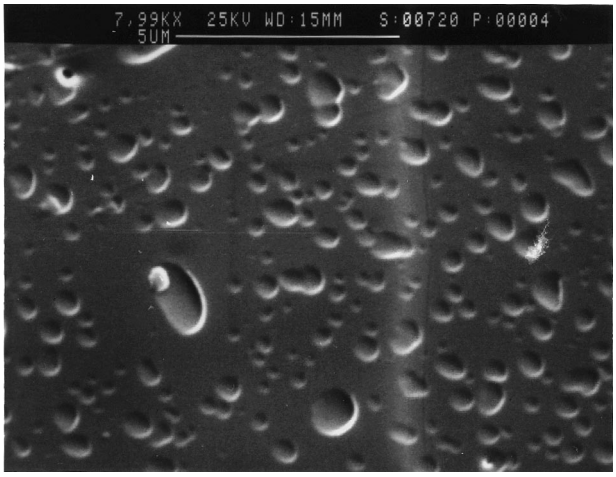

Fig. 4. Scanning electron micrograph for the unfractured surface of the 6F-ETPP-E sample with 10 wt% rubbery phase prepared from a 1:3 mole ratio of TMOS:DMDMOS.

the alkyl groups they contain. Most impressively, more than two-fold increases in toughness were achieved for samples corresponding to 1:1 and 1:3 mole ratios of TMOS:DMDMOS.

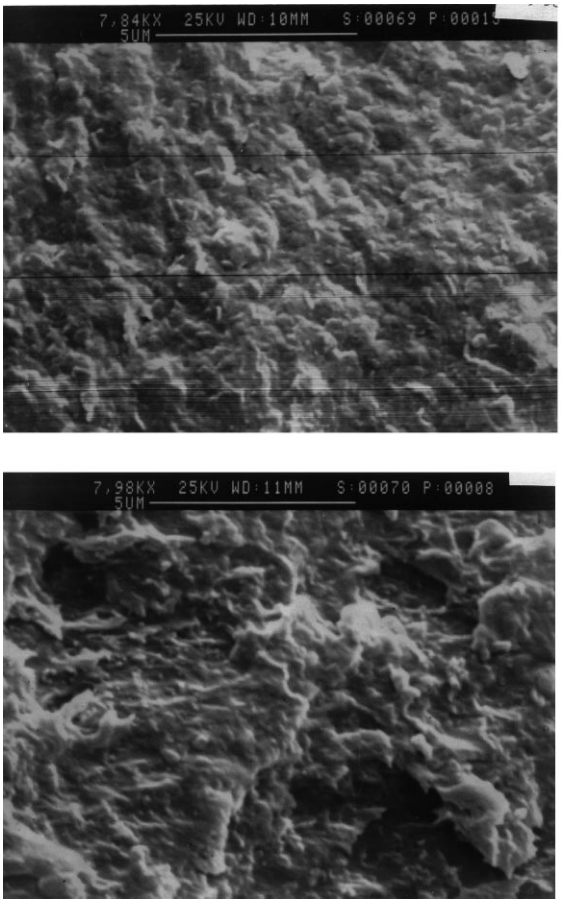

Fig. 5. Scanning electron micrographs for the fractured surface of (a) 6F-ETPP-E pure polymer and (b) the sample with 10 wt% rubbery phase prepared from a 1:1 mole ratio of TMOS:DMDMOS.

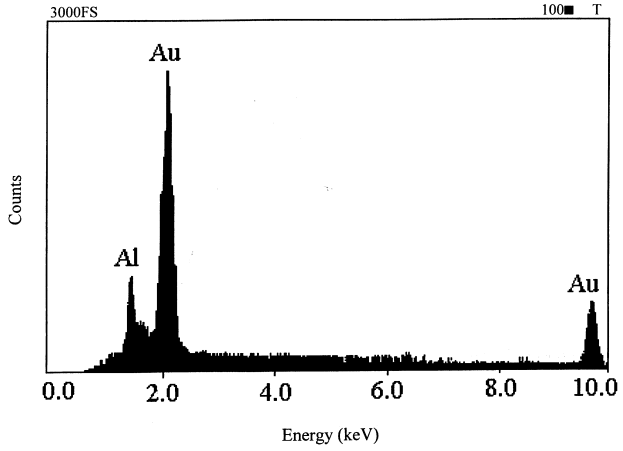

Fig. 6. The EDAX spectrum for the 6F-ETPP-E pure polymer.

The mechanical properties for the FEK-E pure polymer and the samples prepared from it having 10 wt% of the dispersed phase from various TMOS:DMDMOS mole ratios are given in Fig. 10 and Table 5. The sample corresponding to 1:2 mole ratio of TMOS:DMDMOS showed a slight increase in modulus and the other composite samples showed no noticeable change at all. The toughness and ultimate elongation of the sample corresponding to 2:1 mole ratio of TMOS:DMDMOS have been decreased compared to those of the pure polymer. This could be due to the relatively higher amount of silica in the secondary phase in this sample. There is a significant increase in the toughness and ultimate elongation of the samples corresponding to 1:2 and 1:3 mole ratios, however, and this increase is particularly striking for the latter sample. This demonstrates that the larger the number of alkyl groups in the modified dispersed phase, the more pronounced its rubbery properties and therefore the larger the toughening effect.

Fig. 11 and Table 6 describe the mechanical properties of

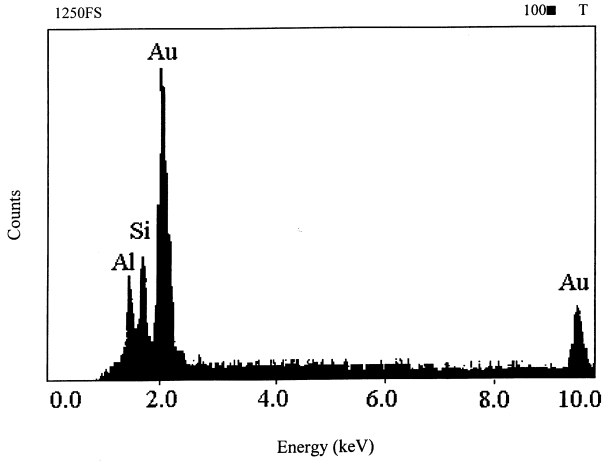

Fig. 7. The EDAX spectrum for the 6F-ETPP-E sample with 10 wt% rubbery phase prepared from a 1:1 mole ratio of TMOS:DMDMOS.

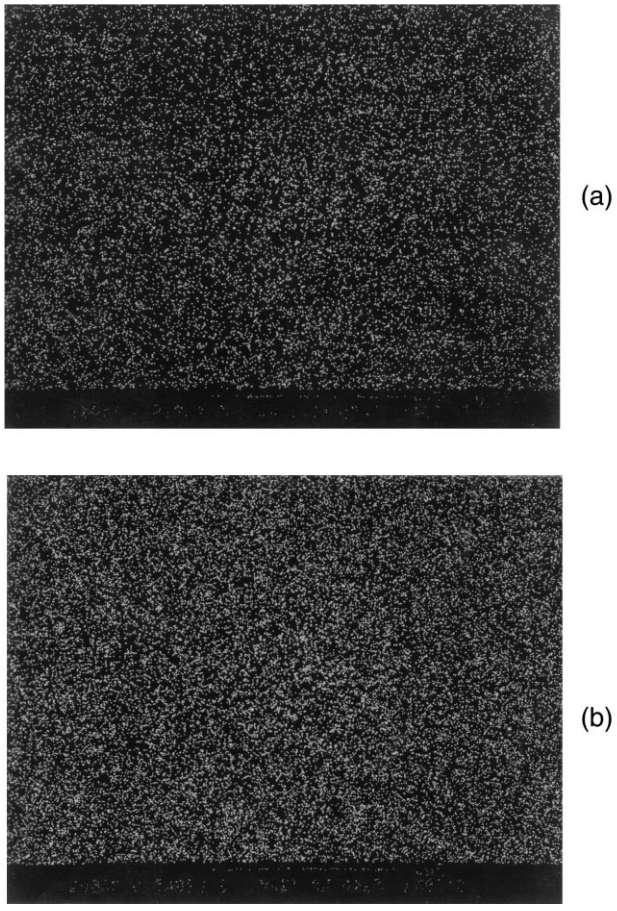

Fig. 8. Silicon distribution maps for the 6F-ETPP-E sample with 10 wt% rubbery phase prepared from a 1:1 mole ratio of TMOS:DMDMOS: (a) unfractured surface and (b) fractured surface.

the HPBO pure polymer and the samples from it containing varying amounts of the rubbery phase from a 1:1 mole ratio of TMOS:MTMOS. There is a slight decrease in moduli of these samples compared to that of the pure polymer. Incorporation of the rubbery phase into the HPBO polymer,

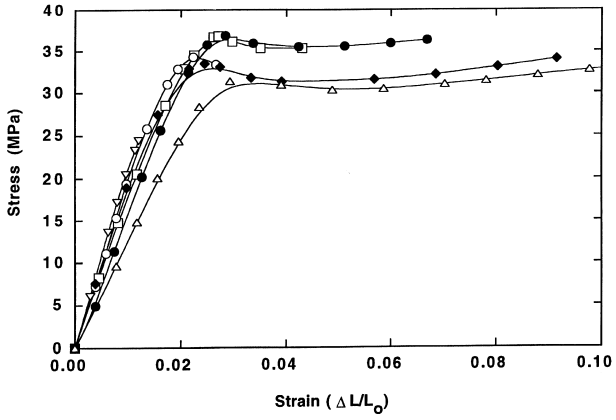

Fig. 9. Stress–strain curves for 6F-ETPP-E pure polymer (□), and for samples containing 10 wt% rubbery phase from 3:1 (△); 2:1 (○), 1:1 (◆), 1:2 (●), and 1:3 (△) TMOS:DMDMOS mole ratios.

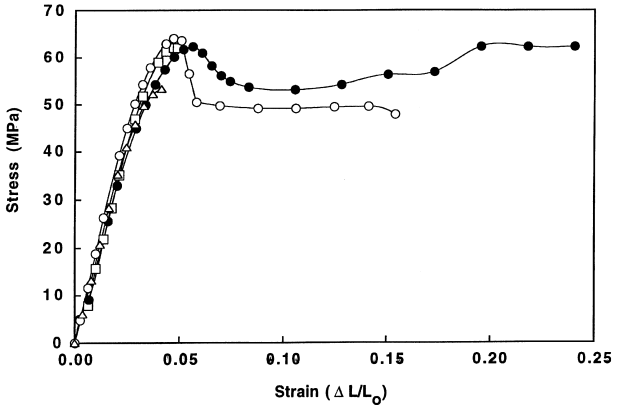

Fig. 10. Stress–strain curves for FEK-E pure polymer (□) and for samples containing 10 wt% rubbery phase from 2:1 (△), 1:2 (○), and 1:3 (●) TMOS:DMDMOS mole ratios.

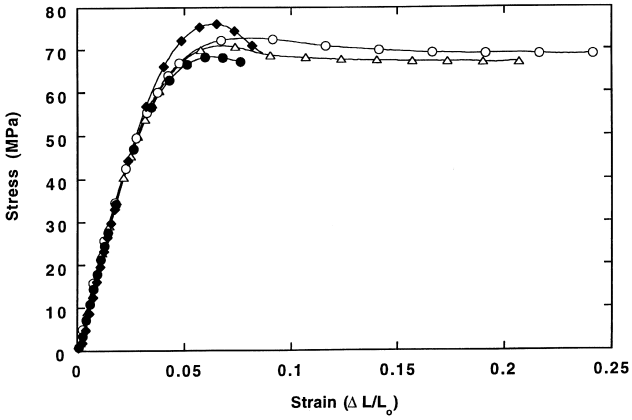

Fig. 11. Stress–strain curves for HPBO pure polymer (◆) and for samples from a 1:1 mole ratio of TMOS:MTMOS with: 5 (△), 15 (○), and 20 wt% (●) rubbery phase.

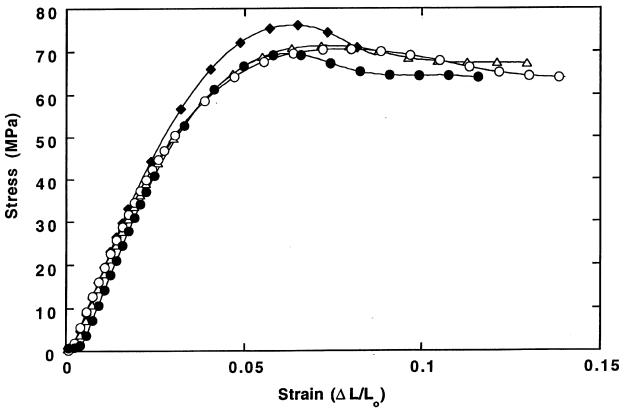

Fig. 12. Stress–strain curves for HPBO pure polymer (◆) and for samples from a 1:1:1 TMOS:DMDMOS:MTMOS mole ratio: 5 (△), 15 (○), and 20 wt% (●) rubbery phase.

Table 5
Mechanical properties of the FEK-E composites

Rubbery phase		Modulus (MPa)	Ultimate strength (MPa)	Ultimate elongation (%)	Toughness (MPa)
Wt%	Sol–gel precursor[a]				
0	–	1630	62.2	4.9	1.62
10	TMOS:DMDMOS (2:1)	1670	53.1	4.2	1.41
10	TMOS:DMDMOS (1:2)	1890	47.9	15.5	6.39
10	TMOS:DMDMOS (1:3)	1670	62.4	24.7	11.1

[a] Molar ratios of the corresponding precursors are given in parentheses.

Table 6
Mechanical properties of the HPNO composites

Rubber phase		Modulus (MPa)	Ultimate strength (MPa)	Ultimate elongation (%)	Toughness (MPa)
Wt%	Sol–gel precursors[a]				
0	–	2140	69.1	8.9	4.95
5	TMOS:MTMOS (1:1)	2040	66.7	20.9	12.8
15	TMOS:MTMOS (1:1)	2120	68.7	24.3	15.8
20	TMOS:MTMOS (1:1)	2050	67.0	7.6	3.84
5	TMOS:DMDMOS:MTMOS (1:1:1)	2100	67.0	13.3	8.08
15	TMOS:DMDMOS:MTMOS (1:1:1)	1980	63.9	14.3	9.28
20	TMOS:DMDMOS:MTMOS (1:1:1)	2070	63.9	11.9	6.37

[a] Molar ratios of the corresponding precursors are given in parentheses.

however, has significantly increased the ultimate elongation and toughness except for the sample having the 20 wt% rubbery phase. The decrease in ultimate elongation and toughness of the sample with the 20 wt% rubbery phase may possibly be due to a relatively large-scale phase separation when large amounts of the second phase are introduced. The ultimate strengths of these materials do not show any obvious trend with increase in the amount of rubbery phase. By incorporating a small amount of the rubbery phase (e.g. 5 wt%), the ultimate elongation and the toughness were increased to a large extent; however, further incorporation of the rubbery phase did not increase the ultimate elongation proportionally. Improvements in ultimate elongation and toughness of the HPBO polymer are rather large compared to that of the 6F-ETPP-E polymer. This may be due to the interfacial bonding between the phases being improved by the use of the bonding agent in the case of the HPBO polymer.

Fig. 12 shows stress–strain curves for some HPBO samples with varying amounts of the second phase, which was generated using all three sol–gel precursors TMOS, MTMOS and DMDMOS in 1:1:1 mole ratio. In this case, the moduli of all three samples having different amounts of rubbery phase were again slightly decreased relative to that of the pure HPBO polymer. However, in

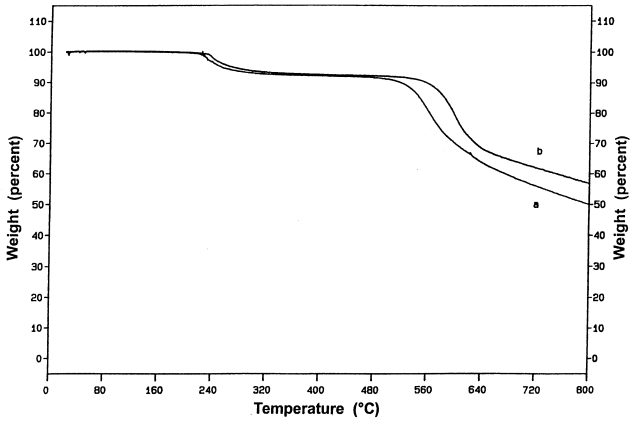

Fig. 13. TGA curves for: (a) FEK-E polymer and (b) its composite having 10 wt% rubbery phase from a 1:3 mole ratio of TMOS:DMDMOS.

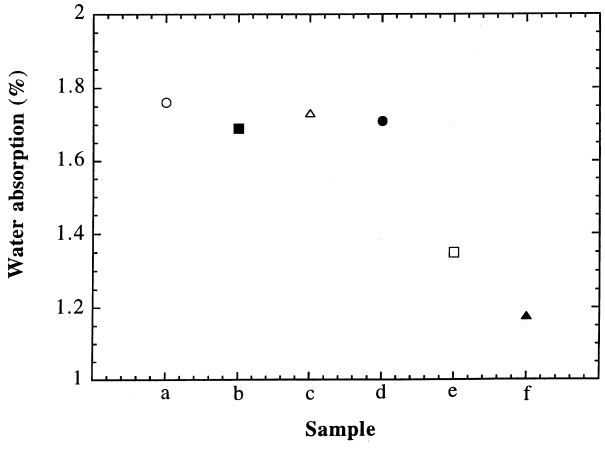

Fig. 14. Extent of water absorption for the 6F-ETPP-E pure polymer (○) and for samples containing 10 wt % rubbery phase from 3:1 (■), 2:1 (△), 1:1 (●), 1:2 (□) and 1:3 (▲) TMOS:DMDMOS mole ratios.

this case the improvements in ultimate elongation and toughness are smaller than in the previous case (with the rubbery phase generated using a 1:1 mole ratio of TMOS:MTMOS).

3.3. Thermal stability

The TGA curves for the FEK-E polymer and its composite having 10 wt% rubbery phase from the 1:3 mole ratio of TMOS:DMDMOS are given in Fig. 13. The temperature at which the drastic weight loss occurs has been raised by about 50°C for this FEK-E composite compared to that for the pure FEK-E polymer suggesting improved thermal stability as measured by TGA through the incorporation of the second phase. In addition, the weight residue at 800°C of this sample is higher compared to that of the pure sample.

3.4. Water absorption

Fig. 14 shows the extent of water absorption for 6F-ETPP-E samples having a 10 wt% rubbery phase. In all the cases, the extent of water absorption is decreased in comparison to that for the pure sample. According to the results, the larger the amount of DMDMOS used relative to TMOS, the lower the water absorptivity. This could be explained by the increased amount of hydrophobic alkyl groups in the samples from the larger amounts of DMDMOS relative to TMOS. The decreased absorption could be very important with regard to dimensional stability and improved dielectric properties.

4. Conclusions

Morphology studies indicated uniformly dispersed rubbery particles in the composites investigated. For the poly(arylene ether)s, a significant increase in toughness and ultimate elongation were achieved for the samples prepared from relatively larger amounts of sol–gel precursors having larger numbers of alkyl groups. In the HPBO samples having low levels of the rubbery phase, both toughness and ultimate elongation were increased with increasing amount of rubbery phase without causing any significant change in the modulus. Improvements in these properties of the HPBO polymer are rather large compared to those of 6F-ETPP-E polymer. This may be due to the interfacial bonding between the phases being improved by the use of the bonding agent in the case of the HPBO polymer. The results also indicated improved thermal properties and decreased water absorption of the composites.

Acknowledgements

It is a pleasure to acknowledge the financial support provided by the Air Force Office of Scientific Research (Directorate of Chemistry and Materials Science) through Grants F49620-96-10052 and F49620-96-10235.

References

[1] Shaw SJ. In: Collyer AA, editor. Rubber toughened engineering plastics. Washington, DC: Chapman and Hall, 1994.
[2] Hodd K. TRIP 1993;1(5):129.
[3] Hergenrother PM. Polym Prepr, Am Chem Soc, Div Polym Chem 1992;33(1):354.
[4] Unroe MR, Gupta RK, Sharma RB, Thiesing NC. Polym Prepr, Am Chem Soc, Div Polym Chem 1997;38(2):293.
[5] Cimmino S, D'Orazio L, Greco R, Maglio G, Malinconico M, Mancarelia C, Martuscelli E, Palumbo R, Ragosta G. Polym Engng Sci 1984;24:48.
[6] Ide F, Hasegawa A. J Appl Polym Sci 1974;18:963.
[7] La Mantia FP, Valenza A. Eur Polym J 1989;24:553.
[8] Li D, Wang H-C, Yee AF. In: Salamone JC, editor. Polymeric materials encyclopedia. Boca Raton, FL: CRC Press, 1996. p. 5409.
[9] Riew CK, editor. Rubber-toughened plastics, vol. 222. Washington, DC: American Chemical Society, 1989.
[10] Riew CK, Kinloch AJ, editors. Toughened plastics I, vol. 233. Washington, DC: American Chemical Society, 1993.
[11] Collyer AA, editor. Rubber-toughened engineering plastics. Washington, DC: Chapman & Hall, 1994.
[12] Ishikawa M. Polymer 1995;36:2203.
[13] Premachandra J, Kumudinie C, Zhao W, Mark JE, Dang TD, Chen JP, Arnold FE. J Sol–Gel Sci Technol 1996;7:163.
[14] Mark JE, Premachandra J, Kumudinie C, Zhao W, Dang TD, Chen JP, Arnold FE. In: Coltrain BK, Sanchez C, Schaefer DW, Wilkes GL, editors. Better ceramics through chemistry VII: organic/inorganic hybrid materials, vol. 435. Pittsburgh, PA: Materials Research Society, 1996. p. 93.
[15] Brinker CJ, Scherer GW. Sol–gel science. New York: Academic Press, 1990.
[16] Mark JE, Lee CY-C, Bianconi PA, editors. Hybrid organic–inorganic composites, vol. 585. Washington, DC: American Chemical Society, 1995.
[17] Mark JE, Wang S, Ahmad Z. Macromol Symp 1995;98:731.
[18] Ahmad Z, Wang S, Mark JE. In: Cheetham A, Brinker CJ, Mecartney ML, Sanchez C, editors. Better ceramics through chemistry VI, vol. 346. Pittsburgh, PA: Materials Research Society, 1994. p. 127.
[19] Premachandra J, Kumudinie C, Mark JE, Dang TD, Arnold FE. J Macromol Sci, Pure Appl Chem 1999;A36(1):73.
[20] Premachandra J, van Ooij WJ, Mark JE. J Adhesion Sci Technol 1998;12(12):1361.
[21] Ning Y-P, Mark JE. Polym Bull 1984;12:407.